Variations in the Tropical Greenhouse Effect during El Niño

BRIAN J. SODEN

Geophysical Fluid Dynamics Laboratory, National Oceanic and Atmospheric Administration, Princeton, New Jersey

(Manuscript received 18 July 1996, in final form 1 October 1996)

ABSTRACT

Observations of the clear-sky outgoing longwave radiation and sea surface temperature are combined to examine the evolution of the tropical greenhouse effect from colder La Niña conditions in early 1985 to warmer El Niño conditions in late 1987. Although comparison of individual months can suggest a decrease in greenhouse trapping from cold to warm conditions, when the entire 4-yr record is considered a distinct increase in tropical-mean greenhouse trapping of $\sim$2 W m^{-2} is observed in conjunction with a $\sim$0.4 K increase in tropical-mean sea surface temperature. This observed increase compares favorably with GCM simulations of the change in the clear-sky greenhouse effect during El Niño–Southern Oscillation (ENSO). Superimposed on top of the SST-driven change in greenhouse trapping are dynamically induced changes in tropical moisture apparently associated with a redistribution of SST during ENSO. The GCM simulations also successfully reproduce this feature, providing reassurance in the ability of GCMs to predict both dynamically and thermodynamically driven changes in greenhouse trapping.

1. Introduction

Water vapor is widely recognized to be a critical component of the climate system. It is the dominant greenhouse gas, trapping more of the earth's heat than any other atmospheric constituent. Water vapor also plays a pivotal role in determining the response of the climate system to increasing greenhouse gases and provides one of the largest known feedback mechanisms for amplifying global warming (IPCC 1990).

Water vapor is generally considered to provide a positive feedback to the climate system (Raval and Ramanathan 1989; Stephens 1990), although there exists some uncertainty regarding the role of upper-tropospheric water vapor (IPCC 1992). Much of this uncertainty stems from limitations in our ability to monitor water vapor in the middle to upper troposphere (Elliott and Gaffen 1990; Soden and Lanzante 1996). Additionally, Lindzen (1990) has suggested that increased convection in a warmer climate would actually dry the upper troposphere by detraining air at higher levels and that existing GCMs are too simplified to adequately represent the effects of convection, such as the detrainment of ice from cumulus towers (Sun and Lindzen 1993), on upper tropospheric moisture. Consequently, he argues, current estimates of global warming are too large. Concern over this issue has stimulated several investigations into the relationship between atmospheric convection and upper-tropospheric moisture (e.g., Rind et al. 1991; Inamdar and Ramanathan 1994; Soden and Fu 1995; Sun and Held 1996) that generally conclude that increased convection results in a moistening of the upper troposphere.

However, the evidence is not unanimous. Recently Chou (1994) analyzed the change in the top-of-atmosphere radiation budget during the 1987 El Niño and found that, when averaged over the tropical Pacific, the clear-sky greenhouse effect was smaller during the warmer month of April 1987 than during the colder month of April 1985. The observed decrease in greenhouse trapping with increased surface temperature was most prominent over the dry subtropical regions and consequently cited as evidence for Lindzen's hypothesis of a negative water vapor feedback.

One possible reason for the apparent discrepancy between Chou (1994) and previous studies is that Chou focused on changes in the radiative energy budget, whereas the previous investigations examined the changes in atmospheric moisture content (e.g., relative or specific humidity). Since the radiative effects are nonlinearly related to the moisture content (Thompson and Warren 1982), it is possible to have an increase in area-mean water vapor associated with a decrease in area-mean radiative trapping.

In this note, the evolution of tropical greenhouse forcing over the course of an El Niño–Southern Oscillation (ENSO) cycle is examined. The variations in greenhouse forcing are shown to closely track the evolution of tropical sea surface temperatures from cold conditions in early 1985 to warm conditions in late 1987. Thus, ob-

Corresponding author address: Dr. Brian J. Soden, GFDL/NOAA, Princeton University, P.O. Box 308, Princeton, NJ 08542.
E-mail: bjs@gfdl.gov

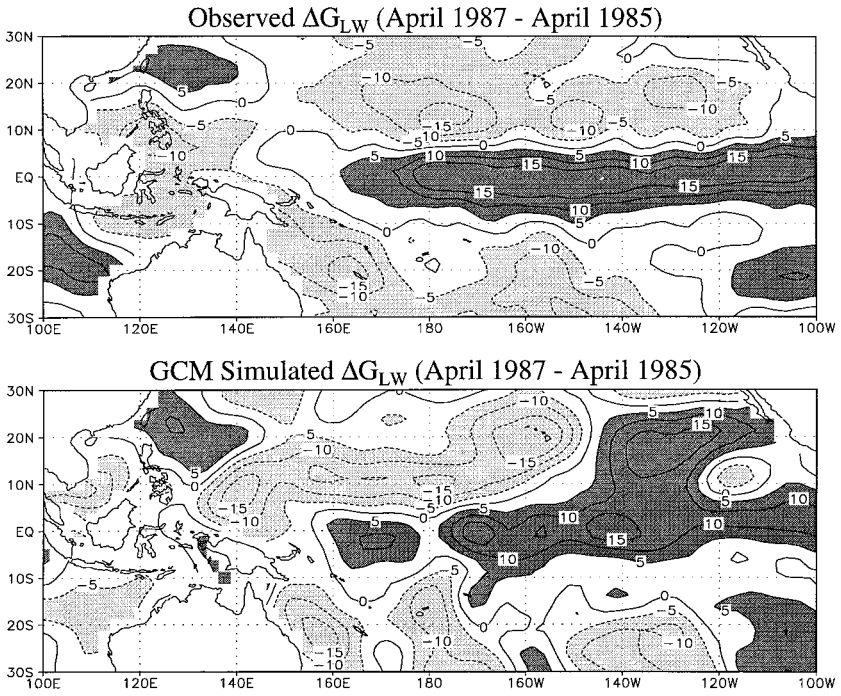

FIG. 1. Map of the difference in greenhouse trapping ΔG_{LW} in W m^{-2} over the tropical Pacific for April 1985–April 1987 from ERBE observations (top) and GFDL GCM simulations (bottom). The contour interval is 5 W m^{-2}. Values greater (less) than 5 W m^{-2} (-5 W m^{-2}) have dark (light) stippling.

servations indicate a positive relationship between SST and greenhouse forcing during ENSO, not a negative relationship as has been previously asserted. Furthermore, this observed relationship is shown to be in close quantitative agreement with that predicted by a GCM, providing reassurance in the ability of GCMs to predict the role of water vapor feedback under global warming scenarios.

2. Observations and model simulations of greenhouse trapping

To examine the change in greenhouse trapping associated with the 1987 ENSO, observations of the outgoing longwave radiation from the Earth Radiation Budget Experiment (ERBE) (Barkstrom et al. 1984) are compared with model simulations using a Geophysical Fluid Dynamics Laboratory (GFDL) general circulation model (GCM). The GCM integrations were performed for 10 yr (1979–88) using observed SSTs as prescribed by the Atmospheric Model Intercomparison Project (Gates 1992). Further details regarding this GFDL GCM can be found in Wetherald et al. (1991). The observed water vapor greenhouse effect ($G_{LW} = \sigma T_s^4 - F_{clr}$) is computed as the difference between the surface emission (σT_s^4) and the clear-sky, top-of-atmosphere outgoing longwave radiation (F_{clr}). Due to inadequate observations of surface temperature over land, calculation of G_{LW} is restricted to oceans using the observed sea surface temperatures of Reynolds (1988). To eliminate the impact of calibration differences in the ERBE longwave channel between individual satellites (Thomas et al. 1995) only measurements from a single satellite, the Earth Radiation Budget Satellite (ERBS), which spans from November 1984 to December 1989, are used here. An identical procedure is used to determine the GCM G_{LW} using the model-calculated F_{clr} and the prescribed sea surface temperatures.

The change in greenhouse trapping associated with tropical warming during the 1987 ENSO can be illustrated by computing the difference in G_{LW} between the warm (El Niño) month of April 1987 and the cold (La Niña) month of April 1985 (Chou 1994). The map of this difference [$\Delta G_{LW} = G_{LW}$ (April 1987) $- G_{LW}$ (April 1985)] for the tropical Pacific is shown in Fig. 1 for both the ERBE observations (top) and GCM simulations (bottom). The observed and GCM-simulated fields of ΔG_{LW} both exhibit an elongated area of enhanced G_{LW} (10 to 15 W m^{-2}) over the central and eastern equatorial Pacific reflecting enhanced moisture over this region due to the eastward shift of convection and the associated change in the Walker circulation. Over the subtropics, both the observations and model simulations generally indicate a decrease in G_{LW} (-10 to -15 W m^{-2}) due to an increase in subsidence and drying of the troposphere over this region. These features are broadly consistent with recent descriptions of the observed changes in tropospheric moisture and tropical circulation during

TABLE 1. The change in tropical-Pacific-mean greenhouse trapping ΔG_{LW} between 1985 and 1987 as a function of month (e.g., April 1987–April 1985, May 1987–May 1985, etc.). For each month the difference ΔG_{LW} is then spatially averaged over the tropical Pacific domain (30°N–30°S, 100°E–100°W) defined by Chou (1994). Results are listed for both the Earth Radiation Budget Experiment (ERBE) observations and GCM simulations.

	ERBE (W m^{-2})	GCM (W m^{-2})
February	−1.9	−0.1
March	+1.1	+0.2
April	−1.2	−0.5
May	+2.0	+0.7
June	+0.8	+1.8

ENSO events (Soden and Fu 1995; Bates et al. 1996; Oort and Yienger 1996). Although there are some regional differences between the observed and predicted ΔG_{LW} (e.g., the eastern subtropical North Atlantic between 10°–25°N and 140°–120°W), overall the anomaly patterns are quite similar.

The patterns of positive and negative anomalies in ΔG_{LW} reflect the changes in tropical circulation associated with ENSO. To assess the net effect of these changes, Chou (1994) averaged the anomalies over the tropical Pacific region, defined as 30°N–30°S and 100°E–100°W, and demonstrated that the tropical-Pacific-mean ΔG_{LW} for ERBE was negative. This suggests that water vapor greenhouse effect decreased in going from the (cold) La Niña to the (warm) El Niño and thus represents evidence of a negative water vapor feedback. These calculations were repeated and confirm that the tropical-Pacific-mean greenhouse trapping decreased by 1.2 W m^{-2} between April 1987 and April 1985 (which is slightly smaller than the difference of 1.3 W m^{-2} reported by Chou, due to the use of only ERBS measurements here). However, it is interesting to note that the simulations performed by the GFDL GCM also indicate a decrease in greenhouse trapping between these two months of 0.5 W m^{-2}, although the magnitude of the decrease is smaller. Nevertheless, the decrease in simulated greenhouse trapping from cold to warm conditions is somewhat surprising since the GCM is known to predict a positive water vapor feedback. The GCM reproduces both the patterns of anomalies in ΔG_{LW} and the sign of the area-mean change yet predicts a positive water vapor feedback; hence, neither the reduction in greenhouse trapping over the subtropics nor the change in Pacific-mean ΔG_{LW} is satisfactory evidence of a negative water vapor feedback.

To examine the sensitivity of this analysis to the month chosen, the difference in tropical-Pacific-mean G_{LW} between 1987 and 1985 was computed for other months besides April and listed in Table 1. The differences show significant month-to-month variability in both sign and magnitude. For example, if one considers May 1987–May 1985 rather than April both the observations and GCM simulations indicate an increase in tropical-Pacific-mean G_{LW}, not a decrease. Similarly, if

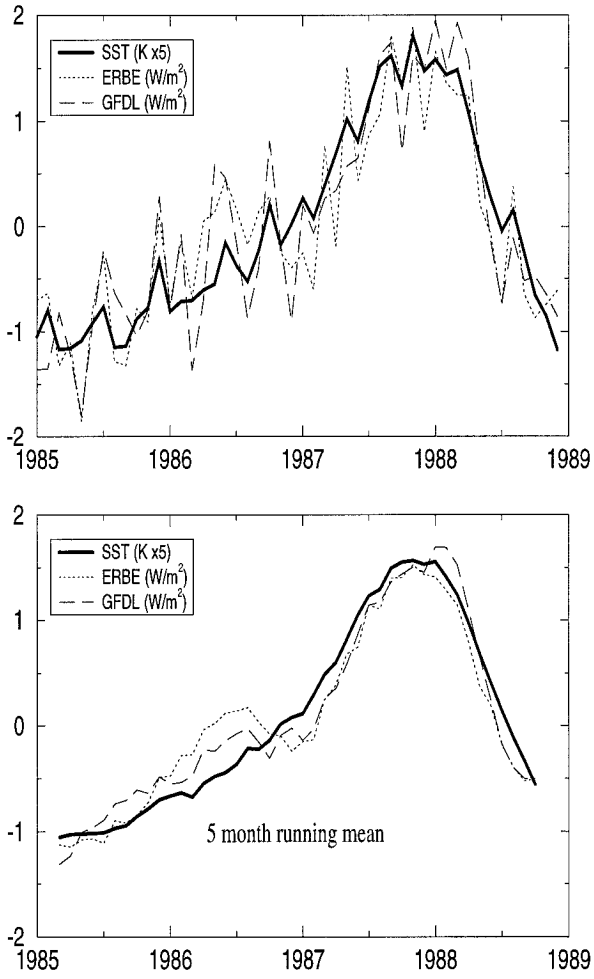

FIG. 2. A time series of the tropical-mean interannual anomaly of greenhouse trapping $\langle \delta G_{LW} \rangle$ (in W m^{-2}) for ERBE observations (dotted line), GFDL GCM simulations (dashed line), and of observed sea surface temperature $\langle \delta SST \rangle$ (in K). The values of $\langle \delta SST \rangle$ are multiplied by 5. The time series in the bottom graph have been smoothed using a 5-month running mean.

March 1987–March 1985 is chosen for the analysis period, the differences are also both positive but considerably smaller than for May. Thus, both sign and magnitude of the differences are strongly dependent upon which pair of months are chosen and conclusions based upon any single pair of months may not be representative of the ENSO event as a whole. Similarly, Hartmann and Michelsen (1993) found that the changes in greenhouse trapping during ENSO can be sensitive to spatial sampling fluctuations and to obtain meaningful results it is necessary to average over the dominant dynamical system of the Tropics, namely the Hadley and Walker circulations.

To obtain a better understanding of how the greenhouse effect over the Tropics evolves throughout the course of the 1987 ENSO, a time series of the interannual anomalies of observed and GCM simulated G_{LW} is plotted in Fig. 2. The interannual anomalies were

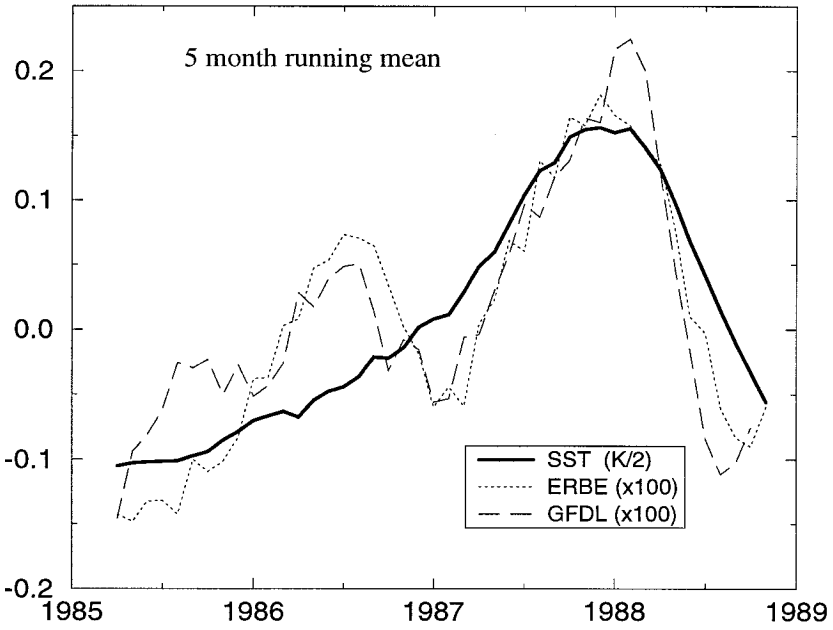

FIG. 3. A time series of the tropical-mean interannual anomaly of fractional greenhouse trapping $\langle \delta g_{LW} \rangle$ (dimensionless) for ERBE observations (dotted line), GFDL GCM simulations (dashed line), and of observed sea surface temperature $\langle \delta SST \rangle$ (in K). The values of $\langle \delta g_{LW} \rangle$ are multiplied by 100 and the values of $\langle \delta SST \rangle$ are divided by 2. All time series have been smoothed using a 5-month running mean.

computed by subtracting the ensemble-mean seasonal cycle from 4 years of data (1985–88) to produce maps of the interannual anomalies δG_{LW}. Since variations in moisture associated with ENSO are not confined to the tropical Pacific but exhibit coherent anomalies that extend throughout the Tropics (Bates et al. 1996; Soden and Bretherton 1996), the anomaly maps were then spatially averaged over the entire tropical belt (30°N–30°S, 0°E–0°W) to yield a tropical-mean interannual anomaly $\langle \delta G_{LW} \rangle$ (''$\langle\ \rangle$'' refers to spatial averaging over the entire Tropics). For comparison purposes, tropical-mean interannual anomalies in sea surface temperature $\langle \delta SST \rangle$ are also shown in Fig. 2 (top). The time series plots confirm that there is a significant amount of month-to-month variability in both the observed and GCM-simulated $\langle \delta G_{LW} \rangle$ even when the spatial averaging is performed over the entire Tropics. Hence, the conclusions obtained by considering only a single pair of months can be misleading.

To remove the large month-to-month variations and focus on the longer term changes, the time series of $\langle \delta G_{LW} \rangle$ and $\langle \delta SST \rangle$ from Fig. 2 (top) were smoothed using a 5-month running-mean and plotted in Fig. 2 (bottom). The chief feature in this plot is the distinct increase in both the observed and GCM-simulated $\langle \delta G_{LW} \rangle$ from approximately -1 W m^{-2} in mid-1985 to approximately $+1$ W m^{-2} in late 1987, followed by a rapid decrease in $\langle \delta G_{LW} \rangle$ to approximately -0.5 W m^{-2} by mid-1988. The changes in greenhouse trapping closely track the changes in $\langle \delta SST \rangle$, which vary by approximately ± 0.2 K over this period. Thus, when the entire time series is considered, the increase in SST during the 1987 ENSO is associated with an increase in G_{LW}, not a decrease as previously asserted. Furthermore, the evolution of GCM-simulated $\langle \delta G_{LW} \rangle$ is remarkably consistent with the observations, which lends credibility to the model's simulation of SST-driven changes in tropical moisture.

Another interesting feature in Fig. 2 is the anomalous increase in the observed $\langle \delta G_{LW} \rangle$ in early 1986 of ~ 0.5 W m^{-2} followed by an anomalous decrease in early 1987 of roughly -0.5 W m^{-2}. Neither of the observed fluctuations coincides with any perceptible change in $\langle \delta SST \rangle$, suggesting that they represent dynamically induced changes in the tropical moisture that, for example, may be associated with the redistribution of SST during ENSO. If this is the case, then the GCM that is forced with observed SSTs should also exhibit these features. Indeed, close inspection of Fig. 2 (bottom) does reveal similar, though somewhat weaker, anomalies in $\langle \delta G_{LW} \rangle$ during 1986–87. Further evidence of the GCM's ability to reproduce this feature is presented below.

Variations in G_{LW} reflect the changes in radiative trapping that arise from both variations in the absorptivity of the atmosphere (e.g., water vapor and lapse rate) as well as variations in the surface emission. To remove the surface emission dependence and focus on changes in atmospheric absorptivity, Raval and Ramanathan (1989) defined a fractional greenhouse trapping $g_{LW} = G_{LW}/\sigma T_s^4$. Figure 3 compares time series of the tropical-

mean interannual anomalies of $\langle \delta g_{LW} \rangle$ from ERBE observations and GCM simulations. Both the observations and model simulations exhibit an increase in $\langle \delta g_{LW} \rangle$ from roughly -0.1 during La Niña conditions in early 1985 to $+0.2$ during El Niño conditions in late 1987 and decrease rapidly thereafter. These changes closely track the tropical-mean SST suggesting that they are largely thermodynamically driven.

In addition to the SST-driven change, the anomalous fluctuations in greenhouse trapping during 1986–87 are much more prominent in $\langle \delta g_{LW} \rangle$. These anomalies in $\langle \delta g_{LW} \rangle$ presumably reflect the impact of dynamically driven changes in atmospheric moisture upon the greenhouse effect. Interestingly, the GCM simulations exhibit a similar oscillation in $\langle \delta g_{LW} \rangle$, both in terms of magnitude and phase. The GCM does predict slightly larger $\langle \delta g_{LW} \rangle$ during 1985; however, overall the similarity between the observed and model-simulated $\langle \delta g_{LW} \rangle$ is quite striking. The lack of correlation with changes in tropical-mean SST suggests that the 1986–87 anomalies are dynamically, rather than thermodynamically, induced (Stephens et al. 1993). This dynamical oscillation is presumably related to the redistribution of tropical SSTs (e.g., Lindzen and Nigam 1987) during the transition from cold to warm conditions. The similarity between the observed and modeled anomalies thus offers encouraging evidence of the GCM's ability to simulate dynamically, as well as thermodynamically, driven changes in tropical greenhouse trapping.

3. Summary

Observations of the outgoing longwave radiation were used to examine the relationship between the clear-sky greenhouse effect and sea surface temperature over the Tropics during the 1987 ENSO and to compare the observed relationship with GCM simulations. The conclusions of this study are summarized as follows.

- A distinct increase in tropical-mean greenhouse forcing $\langle \delta G_{LW} \rangle$ of roughly 2 W m^{-2} is observed in conjunction with the rise in sea surface temperature of $\sim$0.4 K during the evolution from La Niña conditions in early 1985 to El Niño conditions in mid-1988. This change is consistent with a positive relationship between sea surface temperature and greenhouse trapping, not a negative relationship as has been previously suggested.
- The relationship between sea surface temperature and greenhouse forcing predicted by the GFDL GCM is consistent with the observed increase in $\langle \delta G_{LW} \rangle$ of approximately 2 W m^{-2} from La Niña conditions to El Niño conditions.
- Superimposed on top of the SST-driven change in greenhouse trapping are dynamically induced changes in tropical moisture apparently associated with a redistribution of SST during ENSO. The GFDL GCM successfully reproduces this feature.

The relevance of these results to the problem of water vapor feedback obviously depends upon the extent to which ENSO provides a suitable proxy for global warming. Since ENSO represents an internal oscillation of the climate system, whereas global warming results from an external radiative forcing, it is certainly plausible that the relationship between SST and G_{LW} under global warming conditions may differ from that observed here. Rather than speculate along these lines, the objective of this note was to compare the observed relationship between SST and G_{LW} with that simulated by a GCM. Thus, while the observational results presented here may not be directly interpreted as a measure of water vapor feedback, the high degree of similarity between the observed and modeled variations in tropical greenhouse forcing during ENSO provides reassurance in the ability of the GCM to correctly predict this relationship under global warming scenarios.

Acknowledgments. I thank Isaac Held, Steve Klein, Jerry Mahlman, V. Ramaswamy, Pete Robertston, and two anonymous reviewers for commenting on an earlier version of this manuscript; the Langley DAAC for providing the ERBE observations; and Richard Wetherald for providing the GCM simulations.

REFERENCES

Barkstrom, B. R., 1984: The Earth Radiation Budget Experiment (ERBE). *Bull. Amer. Meteor. Soc.,* **65,** 1170–1185.

Bates, J. J., X. Wu, and D. L. Jackson, 1996: Interannual variability of upper troposphere water vapor band brightness temperature. *J. Climate,* **9,** 427–438.

Chou, M. D., 1994: Coolness in the tropical Pacific during an El Niño episode. *J. Climate,* **7,** 1684–1692.

Elliott, W. P., and D. J. Gaffen, 1991: On the utility of radiosonde humidity archives for climate studies. *Bull. Amer. Meteor. Soc.,* **72,** 1507–1520.

Gates, W. L., 1992: AMIP: The Atmospheric Model Intercomparison Project. *Bull. Amer. Meteor. Soc.,* **73,** 791–794.

Hartmann, D. L., and M. L. Michelsen, 1993: Large-scale effects on the regulation of tropical sea surface temperature. *J. Climate,* **6,** 2049–2062.

Inamdar, A. K., and V. Ramanathan, 1994: Physics of the greenhouse effect and convection in warm oceans. *J. Climate,* **7,** 715–731.

IPCC, 1990: *Climate Change: The IPCC Scientific Assessment.* Cambridge University Press, 365 pp.

——, 1992: *The IPCC Supplementary Report.* Cambridge University Press, 200 pp.

Lindzen, R. S., 1990: Some coolness concerning global warming. *Bull. Amer. Meteor. Soc.,* **71,** 288–299.

——, and S. Nigam, 1987: On the role of sea surface temperature gradients in forcing low-level winds and convergence in the tropics. *J. Atmos. Sci.,* **44,** 2418–2436.

Oort, A. H., and J. J. Yienger, 1996: Observed variability in the Hadley circulation and its connection to ENSO. *J. Climate,* **9,** 2751–2767.

Raval, A., and V. Ramanathan, 1989: Observational determination of the greenhouse effect. *Nature,* **342,** 758–762.

Reynolds, R. W., 1988: A real-time global sea surface temperature analysis. *J. Climate,* **1,** 75–86.

Rind, D., E. W. Chiou, W. Chu, J. Larsen, S. Oltmans, J. Lerner, M. P. McCormick, and L. McMaster, 1991: Positive water vapour

feedback in climate models confirmed by satellite data. *Nature,* **349,** 500–503.

Soden, B. J., and R. Fu, 1995: A satellite analysis of deep convection, upper tropospheric humidity, and the greenhouse effect. *J. Climate,* **8,** 2333–2351.

——, and F. P. Bretherton, 1996: Interpretation of TOVS water vapor radiances in terms of layer-average relative humidities: Method and climatology for the upper, middle, and lower troposphere. *J. Geophys. Res.,* **101,** 9333–9343.

——, and J. R. Lanzante, 1996: An assessment of satellite and radiosonde climatologies of upper tropospheric water vapor. *J. Climate,* **9,** 1235–1250.

Stephens, G. L., 1990: On the relationship between water vapor over oceans and sea surface temperature. *J. Climate,* **3,** 634–645.

——, D. A. Randall, I. L. Wittmeyer, D. A. Dazlich, and S. Tjemkes, 1993: The earth's radiation budget and its relation to atmospheric hydrology 3: Comparison of observations over oceans with a GCM. *J. Geophys. Res.,* **99,** 4391–4950.

Sun, D. Z., and R. S. Lindzen, 1993: Distribution of tropical tropospheric water vapor. *J. Atmos. Sci.,* **50,** 1644–1660.

——, and I. M. Held, 1996: A comparison of modeled and observed relationships between interannual variations of water vapor and temperature. *J. Climate,* **9,** 665–675.

Thomas, D., J. P. Duvel, and R. Kandel, 1995: Diurnal bias in calibration of broad-band radiance measurements from space. *IEEE Trans. Geosci. Remote Sens.,* **3,** 670–682.

Thompson, S. L., and S. G. Warren, 1982: Parameterization of outgoing infrared radiation derived from detailed radiative calculations. *J. Atmos. Sci.,* **39,** 2667–2880.

Wetherald, R. T., V. Ramaswamy, and S. Manabe, 1991: A comparative study of the observations of high clouds and simulations by an atmospheric general circulation model. *Climate Dyn.,* **5,** 135–143.